Available online at www.sciencedirect.com
SCIENCE DIRECT
ELSEVIER
International Journal of Mass Spectrometry 249–250 (2006) 45–59
International Journal of Mass Spectrometry
www.elsevier.com/locate/ijms

Structural characterization of peptides via tandem mass spectrometry of their dilithiated monocations

Ping Wang [a], Michael J. Polce [a], Christian Bleiholder [b], Béla Paizs [b], Chrys Wesdemiotis [a,*]

[a] *Department of Chemistry, The University of Akron, Akron, OH 44325-3601, USA*
[b] *Protein Analysis Facility, German Cancer Research Center, Heidelberg, Germany*

Received 13 December 2005; received in revised form 3 January 2006; accepted 3 January 2006
Available online 9 February 2006

Dedicated to the memory of Chava Lifshitz, a close friend and role model. Her numerous pioneering contributions to gas-phase ion chemistry and mass spectrometry will certainly continue to inspire many current and new physical and analytical chemists.

Abstract

A series of singly charged dilithiated peptides $[Pep - H + 2Li]^+$, has been prepared in situ by electrospray ionization (ESI) or matrix-assisted laser desorption ionization (MALDI) and their collisionally activated dissociations (CAD) have been examined by quadrupole ion trap or quadrupole/time-of-flight tandem mass spectrometry, respectively. In the $[Pep - H + 2Li]^+$ derivatives, an acidic proton of the peptide is replaced by a lithium cation, while the other lithium cation provides the charge. Upon CAD, the Li^+ ions become mobile along the backbone of the peptide, inducing fragmentations that produce sequence ions. Density functional theory calculations carried out for the dipeptide complex $[PheGly - H + 2Li]^+$ predict the existence of several isomers, including ions with lithium carboxylate and lithium amide structures with one or two salt bridges. Because the relative energies of these isomers are relatively small, all may be populated upon typical CAD experiments. This explains the presence of protonated, singly lithiated as well as dilithiated fragments in the CAD spectra of $[Pep - H + 2Li]^+$. In general, the CAD spectra contain almost complete, structurally diagnostic y_n^{**}, c_n^{**} and a_n^{*} ion series, which allow for definitive sequence determination (the number of * indicates the number of metal ions in the fragments).

The formation of C- as well as N-terminal products from $[Pep - H + 2Li]^+$ agrees well with both carboxylate and deprotonated amide structures being populated upon CAD, consistent with the theoretical prediction. Besides promoting sequence-specific fragmentations, dilithiation of the precursor ions also enables the elimination of radicals (at low collision energies) to form dilithiated peptide α-backbone radicals. Very similar characteristics are observed for singly charged disodiated peptides.

Keywords: Dilithiated peptides; Peptide sequencing; Peptide radicals; Salt bridges; MS/MS

1. Introduction

Peptide analysis plays an important role in studies aiming at the characterization of protein structure and function. Consequently, the development of effective, rapid and sensitive methods of peptide sequencing has been an active research area in biological science [1–3]. The general protocol for the analysis of protein mixtures by mass spectrometry (MS) begins with separation of the proteins on 2-D gels and subsequent digestion of the individual proteins by trypsin. The digestion products are analyzed by MS to determine their masses. A search of the measured masses in a protein database may help to identify the peptides (and their protein precursor), if that protein had been characterized before [4,5]. Otherwise, the sequences of unknown peptides can be deduced by tandem mass spectrometry (MS/MS) [1–3]. The majority of protein MS and MS/MS studies reported so far have employed fast atom bombardment (FAB) [6], matrix-assisted laser desorption ionization (MALDI) [7,8] or electrospray ionization (ESI) [9] to ionize the digested peptides. FAB was the major ionization method of biological samples in the 1983–1992 decade, while the newer MALDI and ESI methods are largely used today.

In general, the ionization methods mentioned produce protonated peptides $[Pep + H]^+$, having the proton attached at the most basic site of the molecule [10]. Upon collisional excitation, protons not attached to Arg residues become mobile, i.e., they

* Corresponding author. Tel.: +1 330 972 7699; fax: +1 330 972 7370.
E-mail address: wesdemiotis@uakron.edu (C. Wesdemiotis).

1387-3806/$ – see front matter © 2006 Elsevier B.V. All rights reserved.
doi:10.1016/j.ijms.2006.01.003

can move along the backbone or to the side chain substituents to induce fragmentation reactions that yield products characteristic of the peptide sequence [10–14]. Protonated peptides contain three types of backbone bonds, viz. $^{\alpha}C{-}CO$ to $C_{\alpha}{-}CO$ and $N{-}^{\alpha}C$ to $N{-}C_{\alpha}$, all of which may be cleaved upon fragmentation. According to the nomenclature introduced by Roepstorff and Fohlman [15] and later modified by Biemann [16], the resulting fragment ions are classified as a_n, b_n and c_n ions if they retain the N-terminus or x_n, y_n and z_n ions if they retain the C-terminus of the peptide. From these sequence-indicative backbone fragments, the b_n/y_n pairs arising from breakup of the peptide bond usually dominate MS/MS spectra obtained by collisionally activated dissociation (CAD) at low collision energies (eV range) [10–12,14]. The b_n/y_n backbone ions are formed by migration of the ionizing proton to the various N atoms of the amide bonds, which weakens these bonds and facilitates fragmentation via attack of the emerging acylium ions, $C(=O)^{+}\cdots HN$, by a nearby nucleophile [10,11,17–19]. Most often, the attacking nucleophile is the N-terminally adjacent carbonyl oxygen and the b_n product has a protonated oxazolone end group [20,21], while the complementary y_n ion is the protonated form of a truncated peptide [22]. Since such cleavages can take place randomly at any position in the backbone, they lead to complementary series of fragments that reflect the peptide's sequence.

If the peptide carries functionalized amino acid residues (e.g., Asp, His or Lys), certain bonds near these residues may be cleaved preferentially under certain conditions [10,12,23]. Such selective cleavages are of interest because they produce simpler fragmentation patterns in CAD spectra, similar to enzymatic digests producing simpler and more predictable peptide mixtures. For example, it has been found that an internal lysine residue enhances the cleavage of the amide bond in the C-terminal position, especially in the absence of a mobile proton; the amine group of the lysine side chain initiates fragmentation, leading to b_n sequence ions with lactam structures [10,24]. Similarly, in peptides with no mobile proton, acidic residues (Asp, Glu) have been found to enhance cleavage of the C-terminally adjacent amide bond [10,14,25–28]; under these conditions, the acidic proton of the side-chain initiates amide bond cleavage to create a b_n ion with an anhydride end group [14].

Peptides from tryptic digests often yield doubly protonated ions when ionized by ESI, i.e., $[Pep + 2H]^{2+}$. One proton is sequestered at the basic Lys or Arg C-terminal, while the other can migrate along the backbone to produce the same types of ions presented above for singly charged $[Pep + H]^{+}$ ions. It is not uncommon that peptide $[Pep + H]^{+}$ or $[Pep + 2H]^{2+}$ ions do not produce enough backbone fragments upon MS/MS to allow for definitive sequence determination [2]. For this reason, metalated peptides have been investigated as alternative precursor ions [23,24,29–42]. Attachment of a metal cation (M^{+}) to peptides for sequencing purposes can be viewed as "derivatization" of the sample to alter and control the fragmentation observed in MS/MS experiments. Metal ions interact strongly with the basic sites of a peptide molecule, such as the carbonyl groups, N-terminus and side chain substituents. Attachment of a metal ion to a backbone amide group increases the electrophilic character of the amide carbon the same way as proton attachment does, which leads to peptide bond cleavage to yield N-terminal b-type ions or C-terminal y-type ions. Using the nomenclature introduced for protonated fragments, these ions are named $[b_n - H + M]^{+}$ or $[y_n - H + M]^{+}$ ions because they carry M^{+} in place of H^{+} charges; for brevity, the acronyms b_n^{*} and y_n^{*} are used. Peptides cationized by singly charged metal ions undergo a unique fragmentation which produces truncated peptide complexes devoid of the C-terminal amino acid residue; these N-terminal fragments have been termed $[b_{n-1} + OH + M]^{+}$ ions [35]. Because of the favorable energetics of $[b_{n-1} + OH + M]^{+}$ formation, the MS/MS spectra of peptide $[Pep + M]^{+}$ ions are dominated by these fragments and competitive fragmentations are either absent or suppressed significantly [24].

The mechanism of $[b_{n-1} + OH + M]^{+}$ formation has been recently elucidated [43]. This reaction proceeds via a mixed anhydride intermediate. With dipeptides, the same intermediate is traversed irrespective of sequence. As a result, the MS/MS spectra of the $[Pep + M]^{+}$ ions from isomeric dipeptides are often indistinguishable [35,43,44]. Our group recently found that this problem is bypassed if the peptides are derivatized to their carboxylate salts, for example, if $[Pep - H + 2Li]^{+}$ precursor ions are used [44,45]. In the latter complexes, the proton on the C-terminal COOH group is replaced by one lithium cation, while the second lithium cation provides the charge. $[Pep - H + 2Li]^{+}$ ions from isomeric dipeptides (e.g., FG/GF) give substantially different fragmentations patterns, displaying unique c- and y-type fragments that permit unequivocal differentiation [44]. This approach is extended in this study to larger dilithiated peptides. The fragmentation characteristics of a number of $[Pep - H + 2Li]^{+}$ and select $[Pep - H + 2Na]^{+}$ ions are examined in detail by different MS/MS techniques in order to evaluate the usefulness of such precursor ions, vis à vis monometalated or protonated precursor ions, in the elucidation of peptide sequences. The experimental results show that singly charged dimetalated derivatives can lead to valuable sequence insight, which is particularly important when the corresponding protonated or monometalated precursors give MS/MS spectra with incomplete sequence ion series [45].

2. Experimental

2.1. ESI quadrupole ion trap mass spectrometry (QIT MS) experiments

The MS/MS characteristics of $[Pep - H + 2Li]^{+}$ ions formed by ESI were examined by CAD in a Bruker Esquire-LC ion trap (Bruker Daltonics, Billerica, MA). The peptides were dissolved in methanol/water 1:1 (v:v), which was saturated with lithium hydroxide (LiOH) or lithium trifluoroacetate (LiTFA) at a concentration of 1 mg/mL. The solutions were introduced into the ion source by a syringe pump at a rate of 200 μL/h. The spraying needle was grounded and the entrance of the sampling capillary was set at −4 kV. Nitrogen was used as the nebulizing gas (10 psi) and drying gas (8 L/min, 150 °C). $[Pep - H + 2Na]^{+}$ ions were formed analogously, using the corresponding sodium salts. These solutions coproduced $[Pep + H]^{+}$, $[Pep + M]^{+}$ and $[Pep - 2H + 3M]^{+}$ ions. In MS/MS mode, the desired precursor

ion was selected by ejecting all other ions from the trap, and the selected ion was accelerated to undergo CAD with the He buffer gas in the trap by an RF field that was turned on for 40 ms at an amplitude (V_{p-p}) of 0.75–0.95 V. Thirty scans were averaged per spectrum.

2.2. MALDI quadrupole/time-of-flight (Q/ToF) mass spectrometry

A Waters Q/ToF Ultima MALDI mass spectrometer (Waters, Beverly, MA) was used for acquiring MS/MS spectra of MALDI-generated $[Pep - H + 2Li]^+$ complexes. The peptides, LiTFA and the matrix (2′,4′,6′-trihydroxyacetophenone, THAP) were dissolved in acetonitrile/water 3:7 (v:v) at concentrations of 10, 10 and 20 mg/mL, respectively. Sample solutions were made by mixing matrix/salt/peptide solutions in the ratio of 5:1:1. Approximately 1 μL of the well-mixed sample solution was spotted onto a 96-well target and allowed to air dry before introduction into the mass spectrometer. MS/MS spectra were measured by selecting the desired $[Pep - H + 2Li]^+$ ion with the quadrupole and subjecting it to CAD in a hexapole collision cell at a collision energy (laboratory frame) of 45–55 eV. The fragment ions were subsequently sent through the orthogonal ToF section for mass analysis and detection. Argon was used as collision gas at a pressure of 1.85×10^{-5} mbar. Approximately 50 scans were averaged per CAD spectrum.

2.3. Materials

The solvents (HPLC-grade water, acetonitrile and methanol), sodium trifluoroacetate (NaTFA), lithium hydroxide (LiOH) and lithium trifluoroacetate (LiTFA) were purchased from Sigma–Aldrich (Milwaukee, WI). The peptides LGG, GLA, LGF, GLF, GAY, YGG, GGGG, polyglycine, GGKAA, FFFFF, YGGFL, YAGFL, YGGFLK, YAGFLR, SIKVAV, polyalanine and DRVYIHPF were purchased from Sigma (St. Louis, MO), and AAG and AAAA from BACHEM (King of Prussia, PA). All chemicals were used without further purification.

2.4. Calculations

Molecular dynamics simulations on various forms of the dipeptide complex $[FG - H + 2Li]^+$ were performed using the InsightII program (Biosym Technologies, San Diego, CA) in conjunction with the AMBER force field. The energetically most favorable structures were optimized fully, using the same force fields, and grouped into families of ions with similar torsion angles. The most stable species in these families were then fully optimized at the HF/3-21G and B3LYP/6-31G(d) levels. The Gaussian program [46] was used in the latter calculations.

3. Results and discussion

Singly charged dilithiated or disodiated ions from the following peptides (Pep) were investigated: AGG, LGG, GLA, LGF, GLF, GAY, YGG, GGGG, AAAA, GGGGG, GGKAA, FFFFF, YGGFL, YAGFL, GGGGGG, YGGFLK, YAGFLR, SIKVAV, AAAAAAA, AAAAAAAA and DRVYIHPF. These precursors decompose to form fragment ions that contain either one or two metal ions. For simplicity, such fragments are designated by one or two asterisks, respectively. Thus, a b_n^* ion carries one metal ion and has the composition $[b_n - H + M]^+$, M = Li or Na, whereas a y_n^{**} ion carries two metal ions and has the composition $[y_n - 2H + 2M]^+$.

A common characteristic of the $[Pep - H + 2Li]^+$ complexes studied is that upon low-energy CAD they lose H_2O, NH_3 and CO_2, and produce a-, b-, c-, y- and z-type ions with one (*) or two (**) metal ions attached to them. The dilithiated peptides may also undergo losses of their aromatic side chain(s) to form distonic radical ions carrying Li^+ charge(s) and one unpaired electron at one α-C atom of the peptide backbone. Further, selective cleavages at certain peptide residues are also observed. Different aspects of the detailed fragmentation pathways of dilithiated peptides will be presented in the following sections. The decomposition pathways of the corresponding disodiated species are very similar and will be discussed only briefly.

3.1. Random backbone cleavages

The CAD pathways of protonated peptides that do not have extremely basic or acidic residue(s) occur randomly along the peptide backbone, leading to contiguous series of fragment ions that reveal the sequence. Our results show that singly charged dilithiated peptides without extremely basic or acidic residues follow the same trend.

The ESI-QIT CAD spectra of protonated, monolithiated, singly charged dilithiated, singly charged disodiated and singly charged trilithiated YAGFL (alanine–leucine–enkephalin) are contrasted in Figs. 1 and 2. The b_4/a_4 fragments resulting from the loss of the amino acid leucine from the C-terminus dominate the CAD spectrum of protonated YAGFL in Fig. 1(a). The CAD products of monolithiated YAGFL differ significantly from those of the protonated peptide, in that $[b_n + OH + Li]^+$ ions dominate the spectrum (n = 3–4) and the b_4^*/a_4^* fragments have much lower relative abundances than b_4/a_4 from the protonated precursor, cf. Fig. 1(b) versus Fig. 1(a). With the singly charged dilithiated YAGFL precursor, Fig. 1(c), the CAD spectrum becomes markedly different again, displaying dominant a_4^* ions and relatively abundant c_n^{**} ions. The $[Pep - H + 2Li]^+$ ions studied produce upon CAD in the trap almost complete c_n^{**}, y_n^{**} and a_n^* series, accompanied by less abundant b_n^*/b_n^{**} ions (not all ions are labeled in Fig. 1(c) to avoid crowding). The CAD spectrum measured using MALDI-Q/ToF MS/MS (not shown) contains the same fragments but with more complete sequence ion series (even y_1^{**} is observed), for the ToF mass analyzer discriminates less against low mass ions as compared to the ion trap. CAD was also performed on singly charged disodiated YAGFL; the resulting spectrum (Fig. 2(a)) shows an essentially identical fragmentation pattern as $[Pep - H + 2Li]^+$ (Fig. 1(c)), with formation of a_4^*, which has one metal cation attached to it, as the most abundant fragmentation channel. It has been shown previously that monolithiated and monosodiated peptides decompose through common dissociation pathways under con-

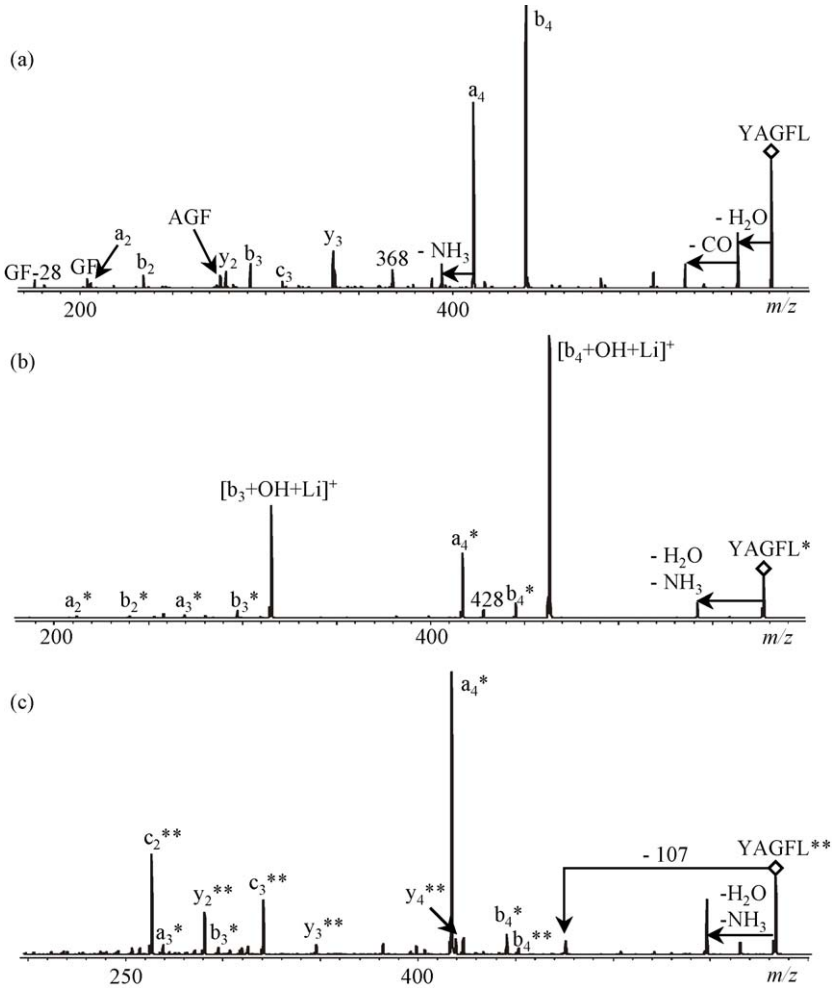

Fig. 1. CAD mass spectra of (a) $[YAGFL + H]^+$ (m/z 570), (b) $[YAGFL + Li]^+$ (m/z 576) and (c) $[YAGFL - H + 2Li]^+$ (m/z 582), acquired using ESI-QIT mass spectrometry.

stant experimental conditions [24]. The results presented here provide evidence that singly charged dilithiated and disodiated peptides decompose through common pathways as well when activated similarly.

Homolytic cleavage reactions also occur in the metalated peptides studied, as attested by the losses of 107 u (*p*-hydroxybenzyl radical) observed in Figs. 1(c) and 2(a). On the other hand, the dominant fragment in the CAD spectrum of trilithiated YAGFL, Fig. 2(b), results from the loss of 4-methylene-2,5-cyclohexadiene-1-one (106 u), i.e., the side chain of Y with one less hydrogen atom, as shown in the spectrum. In this case, the hydrogen in the hydroxyl group is probably replaced by the third lithium ion, which at the same time coordinates to carbonyl groups as well. Upon excitation, the 106-u neutral molecule is eliminated while the lithium cation remains attached to the peptide.

3.2. Structures and decomposition mechanisms of the dilithiated complexes

The $[Pep - H + 2Li]^+$ ions studied correspond to Li^+ complexes of the Li^+ salts of the peptide. Depending on which acidic proton in Pep is replaced by Li^+ ion, several isomeric structures exist for the $[Pep - H + 2Li]^+$ product. In order to determine the most stable conformers, a number of plausible geometries of the dipeptide complex $[FG - H + 2Li]^+$ were optimized by theory. From the families of structures scanned by molecular mechanics/molecular dynamics, those shown in Fig. 3 were found to have the lowest energies. Further optimization and energy minimization of these structures using density functional theory at the B3LYP/6-31G(d) level resulted in the conformations and relative energies summarized in Fig. 3. The most stable $[FG - H + 2Li]^+$ complexes, **1** and **2**, carry both Li^+ cations at the carboxylate group. In conformation **1** (relative energy 0 kJ/mol), one Li^+ is sequestered between the carboxylate oxygens, where it forms a salt bridge, and the second Li^+ is attached to the carbonyl oxygen of the amide bond and the carboxylate oxygen. Both lithium ions are at the same time coordinated by the phenyl ring of the F residue. Alkali metal ions have considerable affinities for aromatic side chain substituents [47,48], and the best possible M^+/aromatic ring interaction is achieved if the metal ion is located above the center of the ring [47]. In such geometry, viz. **2**, only one Li^+ can interact with the phenyl ring, however, resulting in a slightly higher energy (+3 kJ/mol relative to **1**).

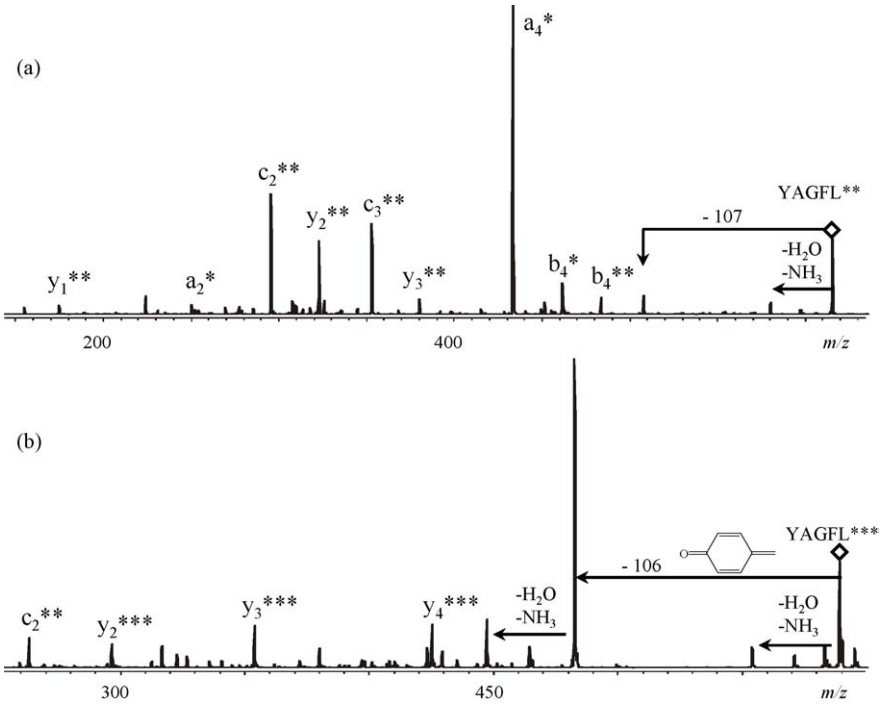

Fig. 2. CAD mass spectra of (a) $[YAGFL - H + 2Na]^+$ (m/z 614) and (b) $[YAGFL - 2H + 3Li]^+$ (m/z 588), acquired using ESI-QIT mass spectrometry.

Tautomeric structures containing deprotonated amide instead of carboxylate groups (**3** and **4**) lie higher in energy, in agreement with the lower acidity of amide versus carboxylic acid substituents (both in the gas-phase [49] and in aqueous solution [50]). Also in these isomers, both Li^+ preferentially attach at the deprotonated anionic center, from where they can simultaneously interact with the functional groups available. In structure **3** (33 kJ/mol relative to structure **1**), one lithium ion interacts with both the C-terminal carbonyl oxygen and the deprotonated amide nitrogen, while the other lithium ion is attached to the deprotonated amide oxygen and the phenyl ring of F. Structure **4** has almost the same energy (36 kJ/mol) as **3**; in this isomer, one lithium ion is coordinated by the C-terminal carbonyl oxygen, the deprotonated amide nitrogen and the aromatic ring and the other lithium cation is attached to the deprotonated amide bond oxygen and the N-terminal amino nitrogen. Structure **5** is a Li-amide and Li-carboxylate structure, in which, according to its name, both the amide nitrogen and the carboxyl group are deprotonated, while the amide oxygen is protonated (two salt bridges). In structure **5**, one lithium cation is attached to both carboxylate oxygen atoms and the other to one carboxylate oxygen, the deprotonated amide nitrogen atom and the aromatic ring of the F residue; further stabilization is incurred by a hydrogen bond between the protonated amide and the N-terminus. The charge-separated structure of FG shown in **5** is a resonance structure of the enol tautomer of the amide group. The energy of structure **5** is only 41 kJ/mol relative to structure **1**; such an energy window is readily accessible in ion trap and Q/ToF instruments, which explains the formation of protonated fragments upon CAD of some singly charged dilithiated peptides.

Plausible structures for the major sequence ions from dilithiated YAGFL are shown in Fig. 4; the ions shown contain two amino acid (AA) residues. The y_n^{**} fragments are dimetalated truncated peptides. Based on the computational results presented above, the most stable and, hence, most likely structure of these ions is a lithium carboxylate structure, such as **1** or **2**. The c_n^{**} series corresponds to the Li^+ complexes of lithium amides. Here, the Li^+ ions are attached to a peptide with an amidated C-terminus. Either the C-terminal or one of the internal amide groups may be deprotonated (the gas-phase acidities of primary and secondary amides are essentially identical [49]). As for the monolithiated a_n^* series, it represents lithiated shorter peptides with imine chain ends, viz. their C-termini carry –CO–N=CHR groups.

Schemes 1–5 provide mechanistic rationalizations for the major fragments formed from collisionally activated YAGFL. These mechanisms are supported by the fragmentations of all dilithiated peptides examined (vide infra) and are helpful for predicting the fragment ions expected from other sequences. The presented mechanisms may not be the lowest energy pathways to the observed products; determining the latter would require elaborate calculations, which are beyond the scope of this study.

According to the DFT calculations on FG, which may be viewed as a model for the C-terminus of YAGFL, the most stable geometry of $[YAGFL - H + 2Li]^+$ should carry both Li^+ ions near the C-terminal carboxylate group. It is proposed that one lithium ion becomes mobile upon CAD, moving to different binding sites along the backbone or at the side chains where, as a Lewis acid, it can promote fragmentation of different bonds. With this assumption, Scheme 1 shows a reaction pathway to y_n^{**} ions, adapted from the established mechanisms operating upon the decomposition of protonated peptides [10,11]. As the mobile Li^+ ion approaches the amide nitrogen of a peptide bond, the carbonyl carbon of this bond becomes more electrophilic,

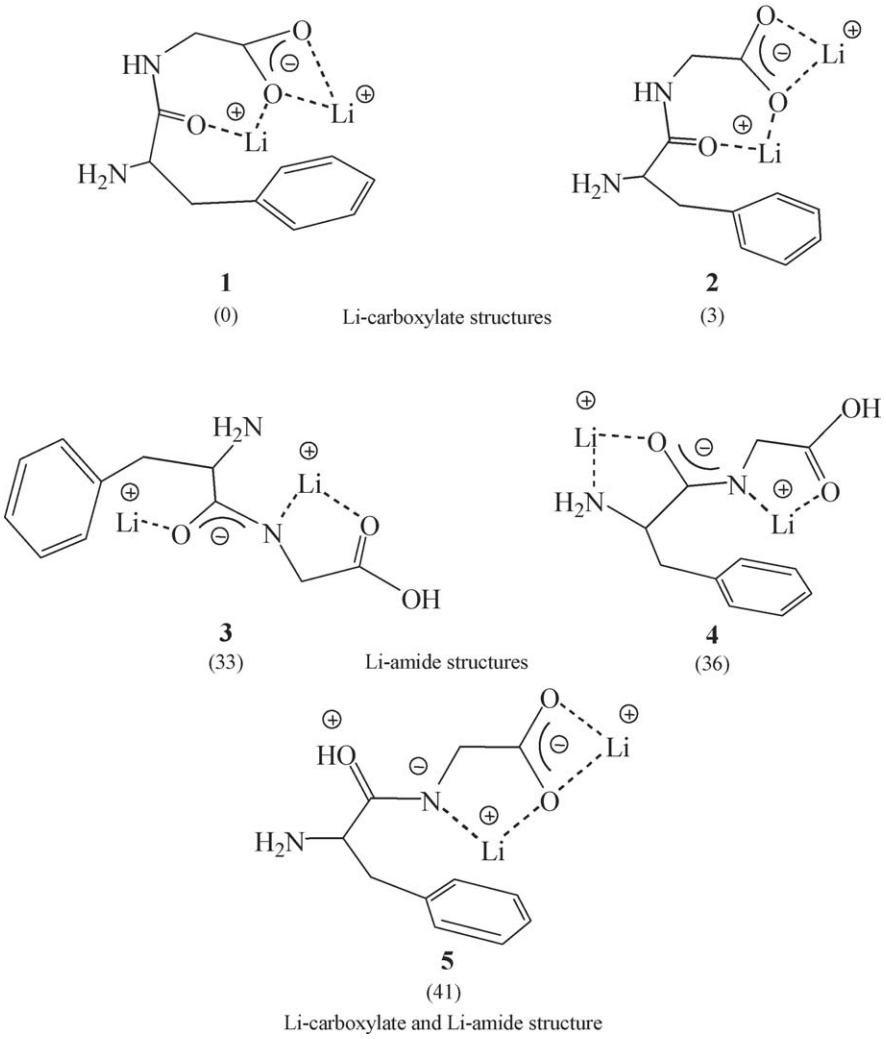

Fig. 3. Most stable isomers and conformers of the $[FG - H + 2Li]^+$ complex, predicted at the B3LYP level of density functional theory. The numbers in parenthesis are relative energies in kJ/mol.

facilitating its attack by the N-terminally adjacent carbonyl oxygen to form a protonated oxazolone. The protonated oxazolone and the detaching Li^+ carboxylate are held together by hydrogen bonding. After proton transfer from the oxazolone to the Li^+ carboxylate piece, the C-terminal part of the peptide is released as a y_n^{**} ion. Scheme 1 illustrates the formation of y_2^{**} ions via this pathway. Li^+ transfer reactions are possible within the ion/molecule complexes emerging after amide bond cleavage. Thus, if the Li^+ ion involved in the dissociation is transferred to the N-terminal oxazolone piece, a b_n^* ion is formed, as illustrated for b_3^* in Scheme 1.

N-terminal c-type ions are usually observed up to c_{n-2}^{**}, which is the c_3^{**} ion from dilithiated YAGFL. In the mechanism proposed in Scheme 2, dissociation to c_{n-2}^{**} begins from a lithium carboxylate structure. Charge-induced bond cleavages, as shown in the Scheme, lead to the expulsion of three stable molecules (viz. CO_2, a ketene and an imine) and the c_3^{**} ion. The formation of c_3^{**} could be promoted by Li^+ attachment at the carboxyl oxygen N-terminal to the N–C_α bond being broken. In the final product, both Li^+ ions have moved away from the C-terminus. The structure shown for c_3^{**} is not necessarily the lowest energy isomer; in the latter, both metal ions are most likely bound near the deprotonated amide group (where the negative charge density is high) and simultaneously interact with other basic sites, such as carbonyl and aromatic groups.

The mechanism outlined in Scheme 2 cleaves the N–C_α bond in the $(n-1)$th AA residue (counting from the N-terminus), giving rise to a c^{**} ion with $n-2$ residues; it cannot produce a c_{n-1}^{**} ion, in accord with the absence of such fragments in the CAD spectra of most dilithiated peptides (vide infra). The formation of $c_{<n-2}^{**}$ ions, on the other hand, can be explained by tautomerization of the lithium carboxylate to a lithium amide structure, prior to charge-induced bond cleavages; Scheme 3 illustrates this case, in which a ketene, an imine and an isocyanate are eliminated to yield a c_2^{**} ion from dilithiated YAGFL. The pathway depicted in Scheme 2 gives rise to the largest c^{**}-type ion observed from most peptides (i.e., c_{n-2}^{**}), while that in Scheme 3, and analogous pathways starting from other deprotonated amide tautomers, give rise to smaller c^{**}-type fragments

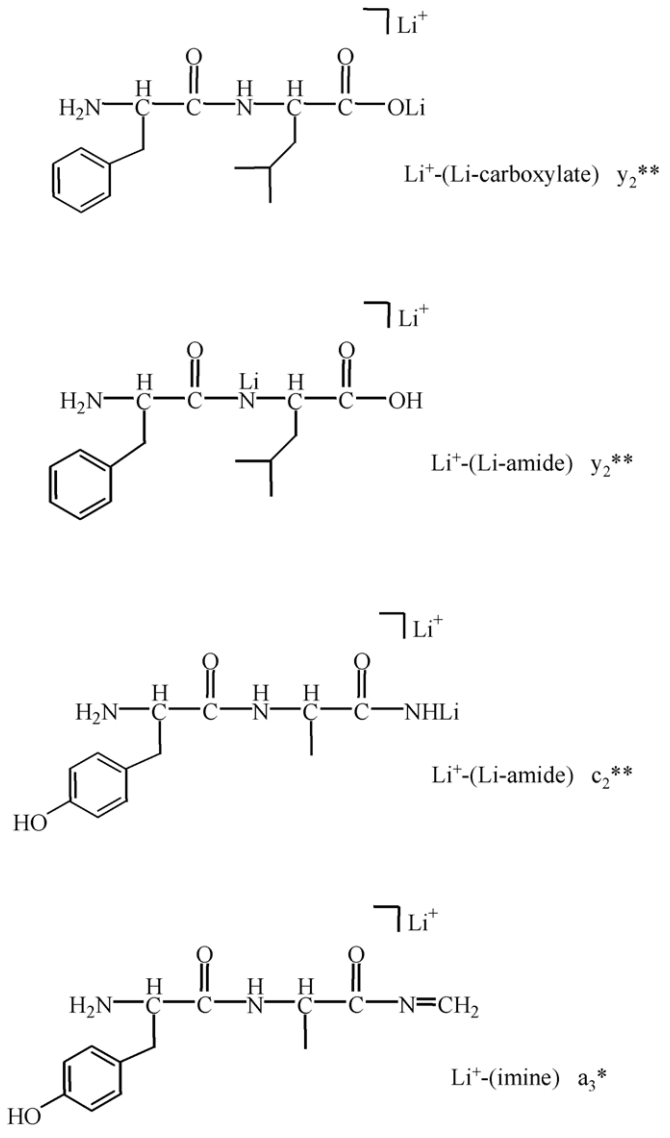

Fig. 4. Major sequence ions from singly charged dilithiated YAGFL.

(vide infra). For brevity, both schemes show concerted elimination of the neutral fragments. More likely, however, these losses (or the losses of isomeric moieties) take place via consecutive reactions involving intermediates.

The much higher relative abundance of y_2^{**} versus b_3^{*} in Fig. 1(c) points out that the lithium carboxylate of the dipeptide FL has a higher Li^+ affinity than the oxazolone-terminated YAG piece. Doubly lithiated b_n^{**} ions are also observed occasionally, in general with lower abundance than b_n^{*}; for example, b_3^{**} appears just above noise level in Fig. 1(c). The formation of such ions nevertheless indicates that the ion/molecule complex produced upon amide bond cleavage is long-lived, allowing for several H^+/Li^+ exchanges between the complex constituents. Note that the nascent y_2^{**} structure arising from amide bond cleavage in Scheme 1 is not the most stable one. As the bond is broken and y_2^{**} departs, rearrangement to the energetically most favorable structure **1**/**2** (Fig. 2) is expected to occur.

Table 1
Important fragment ions formed upon CAD of singly charged dilithiated peptides[a]

Peptide	$a_n/a_n^{*}/a_n^{**}$	$b_n/b_n^{*}/b_n^{**}$	c_n^{*}/c_n^{**}	y_n^{**}
YGGFL	a_3^{*}/a_3^{**}	b_3^{*}/b_3^{**}	c_2^{*}/c_2^{**}	y_2^{**}
	$\mathbf{a_4}^{*}/a_4^{**}$	b_4^{*}/b_4^{**}	c_3^{*}/c_3^{**}	y_3^{**}
				y_4^{**}
AAAAAAAA	a_3^{*}/a_3^{**}	b_3^{*}/b_3^{**}	c_2^{**}	y_3^{**}
	a_4^{*}/a_4^{**}	b_4^{*}/b_4^{**}	c_3^{*}/c_3^{**}	y_4^{**}
	a_5^{*}/a_5^{**}	b_5^{*}/b_5^{**}	c_4^{*}/c_4^{**}	y_5^{**}
	$\mathbf{a_6}^{*}/a_6^{**}$	b_6^{*}/b_6^{**}	c_5^{*}/c_5^{**}	y_6^{**}
	a_7^{*}/a_7^{**}	b_7^{*}/b_7^{**}	c_6^{*}/c_6^{**}	y_7^{**}
AAAAAAA	a_3^{*}/a_3^{**}	b_3^{*}/b_3^{**}	c_2^{*}/c_2^{**}	y_2^{**}
	a_4^{*}/a_4^{**}	b_4^{*}/b_4^{**}	c_3^{*}/c_3^{**}	y_3^{**}
	a_5^{*}/a_5^{**}	b_5^{*}/b_5^{**}	c_4^{*}/c_4^{**}	y_4^{**}
	$\mathbf{a_6}^{*}/a_6^{**}$	b_6^{*}/b_6^{**}	c_5^{*}/c_5^{**}	y_5^{**}
				y_6^{**}
AAAA	a_2^{*}	b_2^{*}	c_2^{**}	y_1^{**}
	$\mathbf{a_3}^{*}/a_3^{**}$	b_3^{*}/b_3^{**}		y_2^{**}
				y_3^{**}
GGGGGG	a_3^{*}	b_2^{*}/b_2^{**}	c_2^{*}/c_2^{**}	y_2^{**}
−18 u	a_4^{*}/a_4^{**}	b_3^{*}/b_3^{**}	c_3^{*}/c_3^{**}	y_3^{**}
	a_5^{*}/a_5^{**}	b_4^{*}/b_4^{**}	c_4^{**}	y_4^{**}
		$b_5^{*}/\mathbf{b_5}^{**}$		y_5^{**}
GGGGG	a_3^{*}	b_3^{*}/b_3^{**}	c_2^{*}/c_2^{**}	y_2^{**}
−18 u	$\mathbf{a_4}^{*}/a_4^{**}$	b_4^{*}/b_4^{**}	c_3^{*}/c_3^{**}	y_3^{**}
				y_4^{**}
GGGG	a_2^{*}	b_2^{*}/b_2^{**}	$\mathbf{c_2}^{**}$[b]	y_1^{**}
−18 u	a_3^{*}	b_3^{*}/b_3^{**}		y_2^{**}
				y_3^{**}
FFFFF	a_2^{*}/a_2^{**}	b_2^{*}/b_2^{**}	c_2^{**}	y_2^{**}
	a_3^{*}/a_3^{**}	b_3^{*}/b_3^{**}	c_3^{**}	y_3^{**}
	$\mathbf{a_4}^{*}/a_4^{**}$	b_4^{*}/b_4^{**}		y_4^{**}
AGG	a_2^{*}		c_1^{**}[c]	y_1^{**}
−18 u				$\mathbf{y_2}^{**}$
GAY[d]	a_2^{*}/a_2^{**}			$\mathbf{y_1}^{**}$
−18 u				y_2^{**}
GLA	a_2[e]$/\mathbf{a_2}^{*}/a_2^{**}$	b_2	c_2^{**}	y_1^{**}
−18 u				y_2^{**}
GLF	$\mathbf{a_2}^{*}/a_2^{**}$		c_2^{**}	y_1^{**}
−18 u				y_2^{**}
LGG	a_2^{*}/a_2^{**}		c_1^{**}[c]	y_1^{**}
−18 u				$\mathbf{y_2}^{**}$
LGF[f]	a_2^{**}	b_2^{*}	$\mathbf{c_1}^{**}$[c]	$\mathbf{y_1}^{**}$
			c_2^{**}	y_2^{**}
YGG[g]	a_2^{*}		c_1^{**}[c]	y_1^{**}
−18 u				$\mathbf{y_2}^{**}$

[a] The most abundant sequence fragment is given in bold. Italicized are fragments with <20% relative intensity in respect to the most abundant sequence ion. The notation −18 u indicates that water loss is the dominant CAD channel (consecutive losses of NH_3, CO or CO_2 also take place).

[b] Isobaric with a_3.

[c] Isobaric with a_2.

[d] This peptide also produces an abundant z_1^{**} ion.

[e] Isobaric with c_1^{**}.

[f] The most abundant CAD fragment (*m*/*z* 188) results from the loss of water and $H_2N–CH(CH_2CH(CH_3)_2)–C(=O)–N=CH_2$) (see Table 3 in [44]).

[g] This peptide also produces an abundant fragment via loss of a $^{\bullet}CH_2–C_6H_4–OH$ radical from the tyrosine side chain.

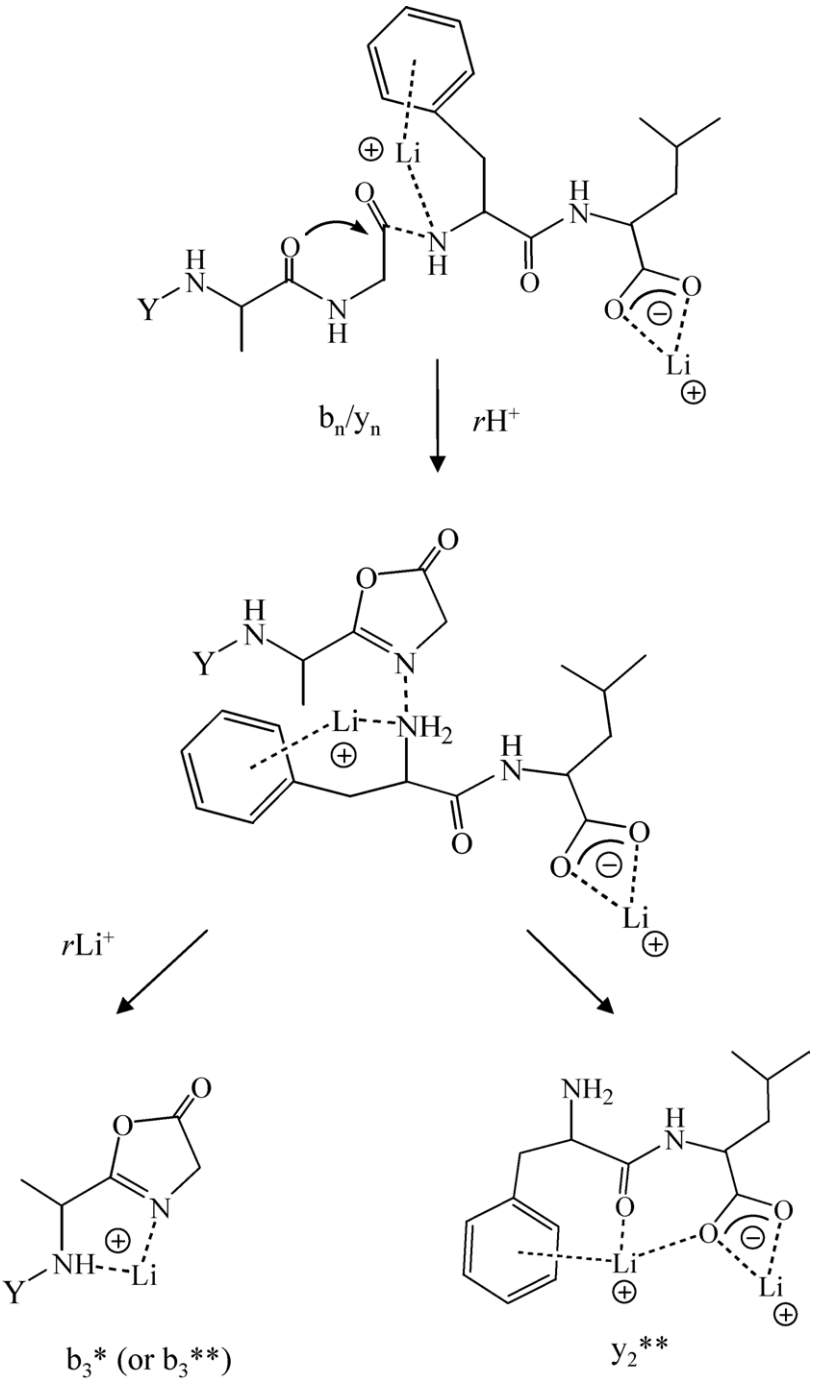

Scheme 1. Dissociation pathway of $[YAGFL - H + 2Li]^+$ to b_n^*/b_n^{**} ($n > 1$) and y_n^{**} ($n < 4$) ions.

The mechanism presented in Scheme 1 is termed the b_n/y_n pathway, in analogy to the b_n/y_n pathway operating in protonated peptides when they dissociate to form b_n and y_n sequence ions [11,17,18]. The b_n/y_n mechanism does not apply to the cleavage of the first N-terminal amide bond, where an oxazolone cannot be formed. This cleavage is explained by an alternative pathway, shown in Scheme 4, and adapted from the a_1/y_{n-1} pathway of protonated peptides [10,11,17,18]. Again, dissociation is promoted by attachment of the mobile Li^+ ion near the amide nitrogen, which elongates the corresponding CO–NH bond, creating an unstable acylium cation that loses CO to form a proton-bound complex between an immonium ion and the detaching Li^+ amide. Proton transfer to the amide gives rise to y_{n-1}^{**} (y_4^{**} from dilithiated YAGFL) and a neutral imine.

Lithium amide structures can be invoked to rationalize the a_n^* series, as shown in Scheme 5. Here, the amide anion induces bond cleavages towards the C-terminal side (in contrast to the mechanism in Scheme 3), leading to the expulsion of CO and, after proton transfer between the dissociating segments, to the formation of a_n^* and a neutral lithium carboxylate salt.

Table 1 summarizes the CAD spectra of the $[Pep - H + 2Li]^+$ ions studied. Most fragments contain one or two Li^+ ions, in

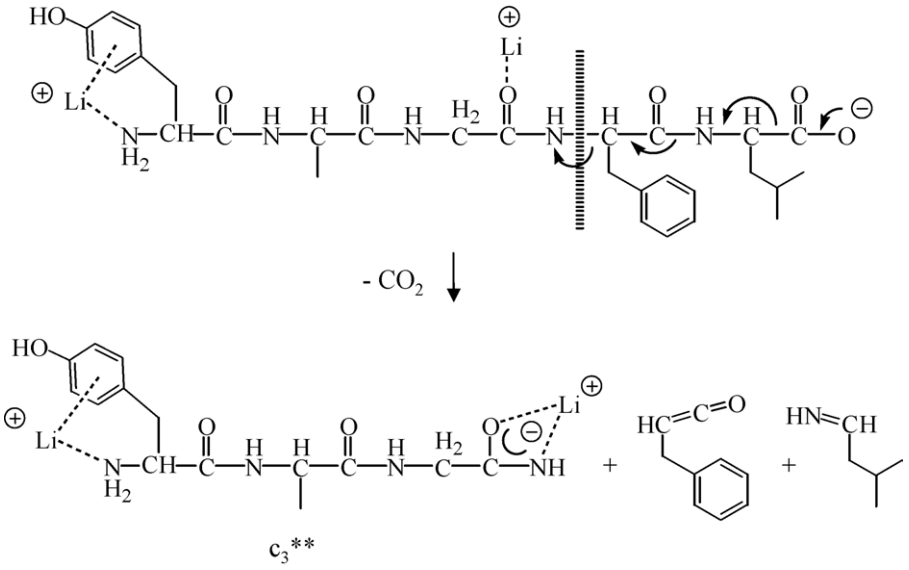

Scheme 2. Dissociation pathway of $[YAGFL - H + 2Li]^+$ to c_{n-2}^{**} (i.e., c_3^{**}) ions.

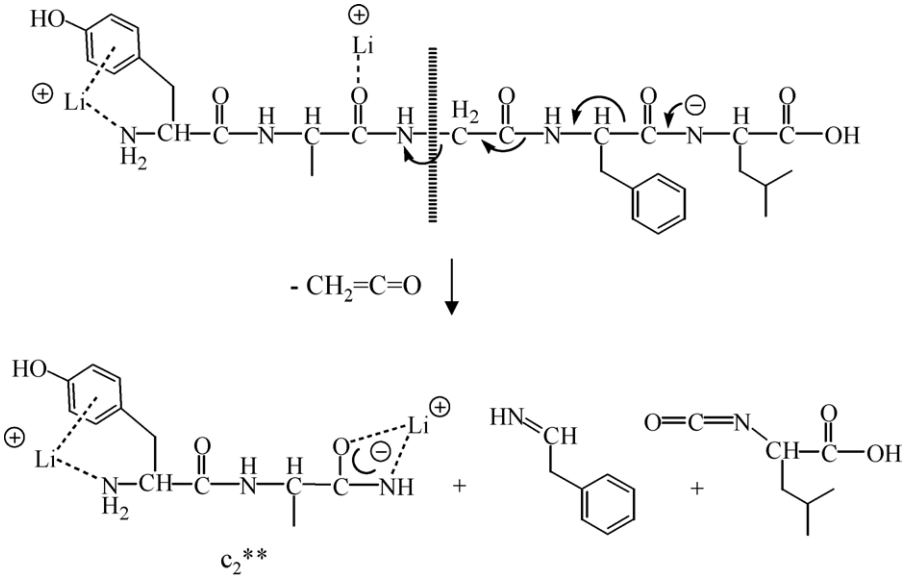

Scheme 3. Dissociation pathway of $[YAGFL - H + 2Li]^+$ to $c_{<n-2}^{**}$ ions.

agreement with the pathways presented in Schemes 1–5. Protonated species (i.e., no Li^+ content) are, however, also observed, especially from some of the smaller peptides. This finding affirms that the dissociations proceed through ion/molecule complexes, as has been mentioned, in which H^+/Li^+ exchange reactions are possible.

Remarkable differences are observed in the relative abundances of a_2^* in the CAD spectra of the dilithiated tripeptides. While GLA, GLF and GAY give rise to intense a_2^* ions, AGG, LGG, LGF and YGG produce much less or no a_2^*. This result suggests that cleavages C-terminal to glycine residues (cf. Scheme 5) are less competitive. Also in protonated peptides, bond scissions next to glycine residues are inefficient [51].

A few tripeptides produce N-terminal c_{n-1}^{**} fragments (i.e., c_2^{**}) in low yield; with all other peptides discussed so far, c_{n-2}^{**} was the largest c^{**}-type ion formed upon CAD (Table 1). A plausible pathway to c_{n-1}^{**} is given in Scheme 6 for $[GLA - H + 2Li]^+$. It begins with CO_2 elimination from the carboxylate tautomer and continues with expulsion of an olefin from the C-terminal residue, which requires proton shift from the side chain. In support of this proposition, only peptides with a side chain at their C-terminal residue undergo this reaction (GLA, GLF and LGF in Table 1); a very similar mechanism was proposed for the formation of c_{n-1}^{**} ions from dilithiated dipeptides carrying a side chain in C-terminal position [44]. When observed (from tri- or larger peptides), c_{n-1}^{**} ions have low relative abundances, suggesting that their formation (Scheme 6) is associated with less favorable energetics as compared to the formation of smaller c^{**}-type or other sequence ions (Schemes 1–5).

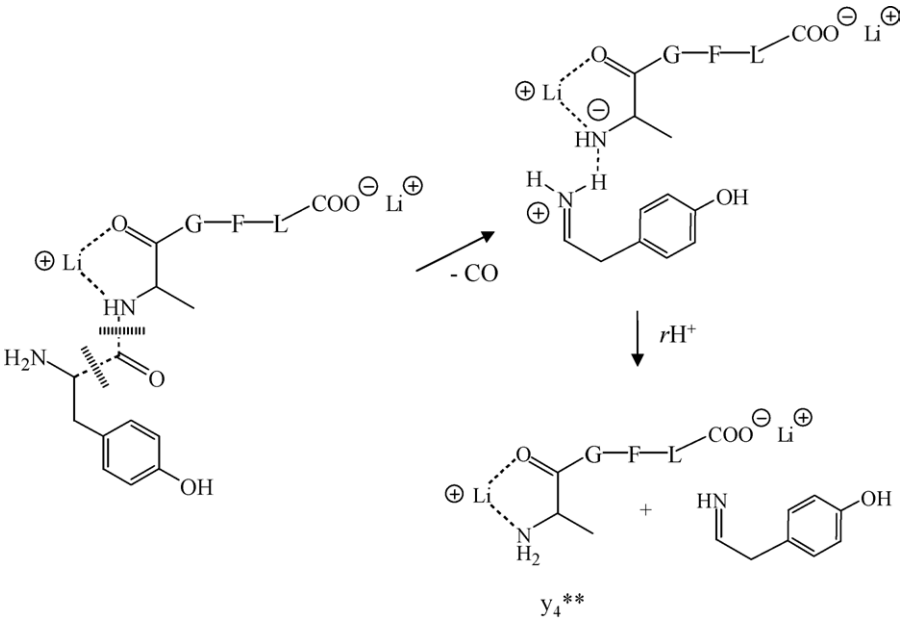

Scheme 4. Dissociation pathway of $[YAGFL - H + 2Li]^+$ to y_{n-1}^{**} (i.e., y_4^{**}) ions.

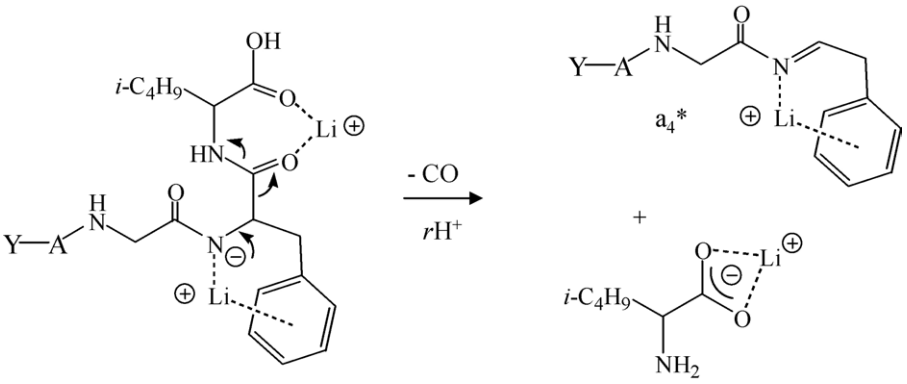

Scheme 5. Dissociation pathway of $[YAGFL - H + 2Li]^+$ to a_n^* ions.

3.3. Selective cleavage at internal lysine residues

Selective backbone cleavages take place only next to specific residues, under defined conditions. They thus reveal specific structural (sequence) motifs. It has recently been reported that peptide ions with no mobile proton undergo selective cleavage C-terminal to an internal lysine residue [24]. This reaction is catalyzed by the NH_2 group in lysine's side chain (see Scheme 3 in ref. [24]). When singly charged dilithiated GGKAA is subjected to CAD in the ion trap instrument, the formation of b_3^* ions is significantly enhanced (Fig. 5(a)). Now, b_3^* is the dominant peak in the spectrum, in contrast to Fig. 1(c), in which

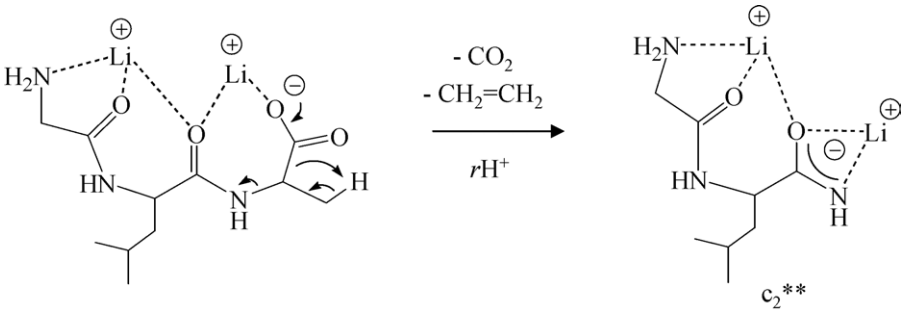

Scheme 6. Dissociation pathway of $[GLA - H + 2Li]^+$ to c_{n-1}^{**} (i.e., c_2^{**}) ions.

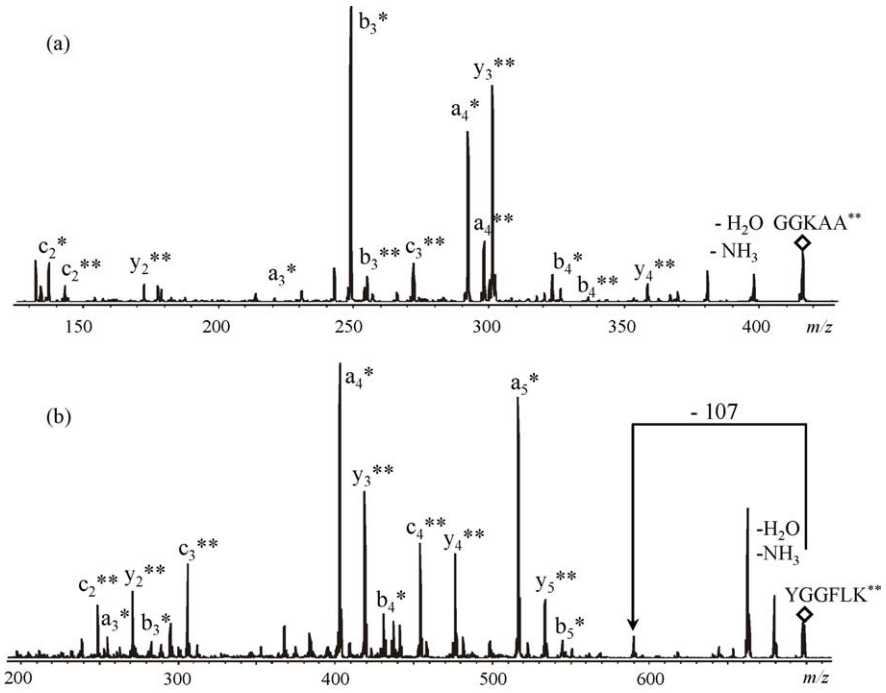

Fig. 5. CAD mass spectra of (a) $[GGKAA - H + 2Li]^+$ (m/z 415) and (b) $[YGGFLK - H + 2Li]^+$ (m/z 696), acquired using ESI-QIT mass spectrometry.

b_3^* is a minor peak. On the contrary, a lysine residue at the C-terminal of the peptide, as in YGGFLK, does not induce a selective cleavage, as is evident from Fig. 5(b). The dominant peaks in the CAD spectrum of YGGFLK** (dilithiated) are c_n^{**}, y_n^{**} and a_n^*, while the b_n^* series is insignificant. These characteristics, which allow definitive sequence determination of the peptide, are very similar to those of YAGFL** (Fig. 1(c)) and YGGFL** (Table 1) which lack a K residue.

3.4. Side chain loss from serine residues

Peptides that have serine residues are believed to undergo side-chain cleavages upon excitation in the mass spectrometer [2,52]. Fig. 6(a) depicts the CAD spectrum of monolithiated SIKVAV, in which the dominant peak is the $[b_5 + OH + Li]^+$ ion that arises from the loss of the C-terminal V residue [24]. This fragment, the parent ion, and a_4^* lose a 30-u neutral (CH_2O), which originates from the side chain of serine, as proved by Adams and co-workers using deuteron labeling experiments [52]. The b_3^* ion is the most abundant b_n^* fragment due to the selective cleavage caused by the internal Lys residue, as mentioned above. Compared to monolithiated SIKVAV, singly charged dilithiated SIKVAV shows more side-chain losses from the serine residue upon CAD, as indicated in the spectrum of Fig. 6(b). It is evident that the major reaction pathway upon excitation of SIKVAV** is loss of 30 u from the parent ion, which corresponds to elimination of the serine side chain. The a_n^* fragments ($n = 4$–5) also undergo 30-u losses; in fact, the $a_n^* - 30$ peaks are more abundant than the a_n^* peaks. The losses of small molecules (e.g., H_2O and NH_3) are also quite abundant compared to other fragmentation pathways. It is noteworthy that C-terminal y_n^{**} ions are formed with measurable abundances from singly charged dilithiated SIKVAV, while y_n^* ions are barely observed from monolithiated SIKVAV. The CAD spectrum acquired using the MALDI-Q-ToF mass spectrometer (not shown) is essentially identical, except that the sequence ions and their consecutive fragments (−30 u) appear with higher relative abundances. The relative abundance of b_3^* (selective cleavage) is low, but it is still higher than those of any other b-type ions formed. The low proportion of b- and c-type fragments from SIKVAV** probably results from the other reaction channels having more competitive kinetics.

Water loss from both monolithiated and dilithiated SIKVAV and their fragments is not as abundant as from protonated serine-containing peptides [2,24]. Conversely, the elimination of CH_2O (30 u) is insignificant for protonated SIKVAV, but considerable for monolithiated and, especially, dilithiated SIKVAV. It is possible that a Li^+ ion replaces the OH proton of the serine side chain in the reacting isomer leading to $CH_2{=}O$ expulsion, thereby facilitating this reaction. The OH → OLi conversion would be more probable in the dilithiated peptide, in agreement with the increased yield of 30-u losses from the latter parent ion.

3.5. Selective cleavage at aspartic acid residues

Protonated peptides with no mobile proton have been known to undergo selective cleavages C-terminal to acidic residues [10,14,28]. In this study, the singly charged dilithiated DRVY-IHPF complex was examined by using both ESI-QIT and MALDI-Q/ToF mass spectrometry. The CAD spectrum of DRVYIHPF** acquired by ESI-QIT MS is shown in Fig. 7(a). The prevailing reaction pathways of this complex are eliminations of stable small molecules, H_2O and NH_3. The next most noticeable peak is y_7^{**} which arises from selective cleav-

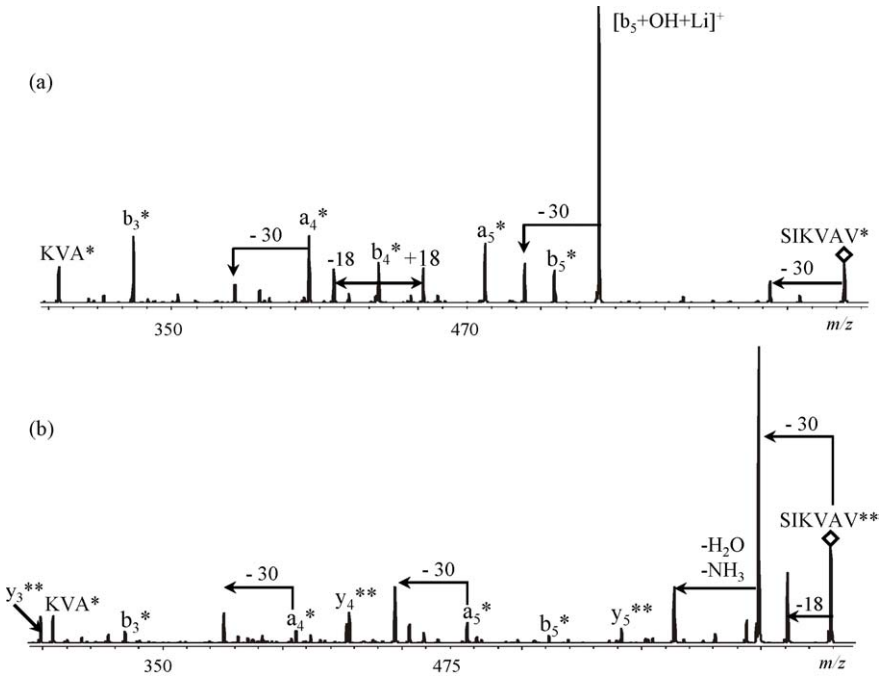

Fig. 6. CAD mass spectra of (a) $[SIKVAV + Li]^+$ (m/z 622) and (b) $[SIKVAV - H + 2Li]^+$ (m/z 628), acquired using ESI-QIT mass spectrometry.

age C-terminal to the aspartic acid residue. Upon CAD in the MALDI-Q/ToF instrument at 55 eV collision energy (laboratory frame), an almost complete y_n^{**} series is obtained (Fig. 7(b)) and other ion series rise slightly above noise level, which provides more information about the peptide sequence. CAD in the MALDI-Q/ToF instrument deposits broader internal energy distributions and higher average internal energies than CAD in an ion trap which, in certain cases (as shown here), leads to structurally more revealing data.

3.6. Peptides with C-terminal arginine residues

The protonated forms of peptides with Arg at their C-termini undergo abundant 60-u losses from the arginine side chain when

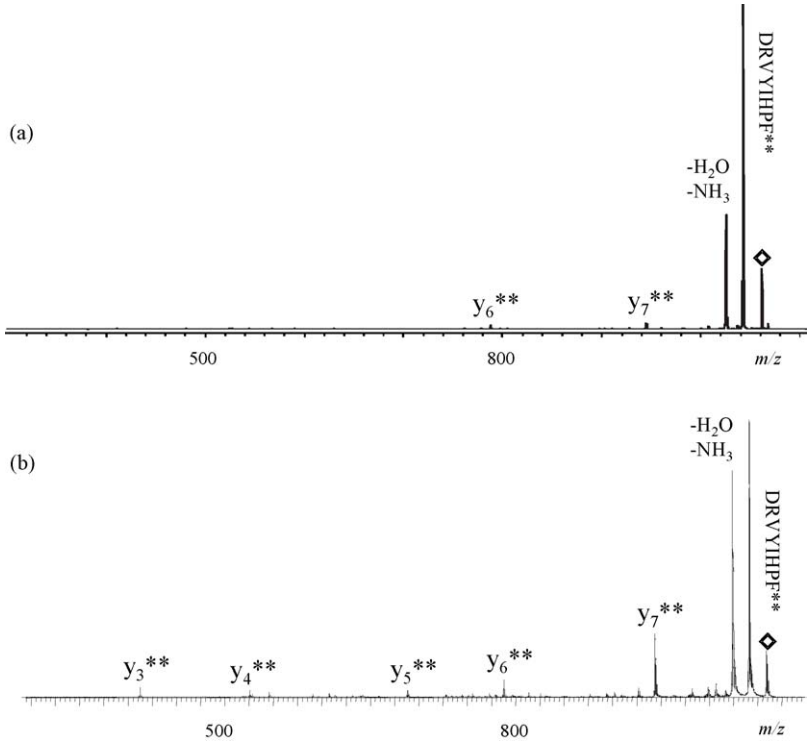

Fig. 7. CAD mass spectra of $[DRVYIHPF - H + 2Li] +$ (m/z 1058), acquired using (a) ESI-QIT and (b) MALDI-Q/ToF mass spectrometry.

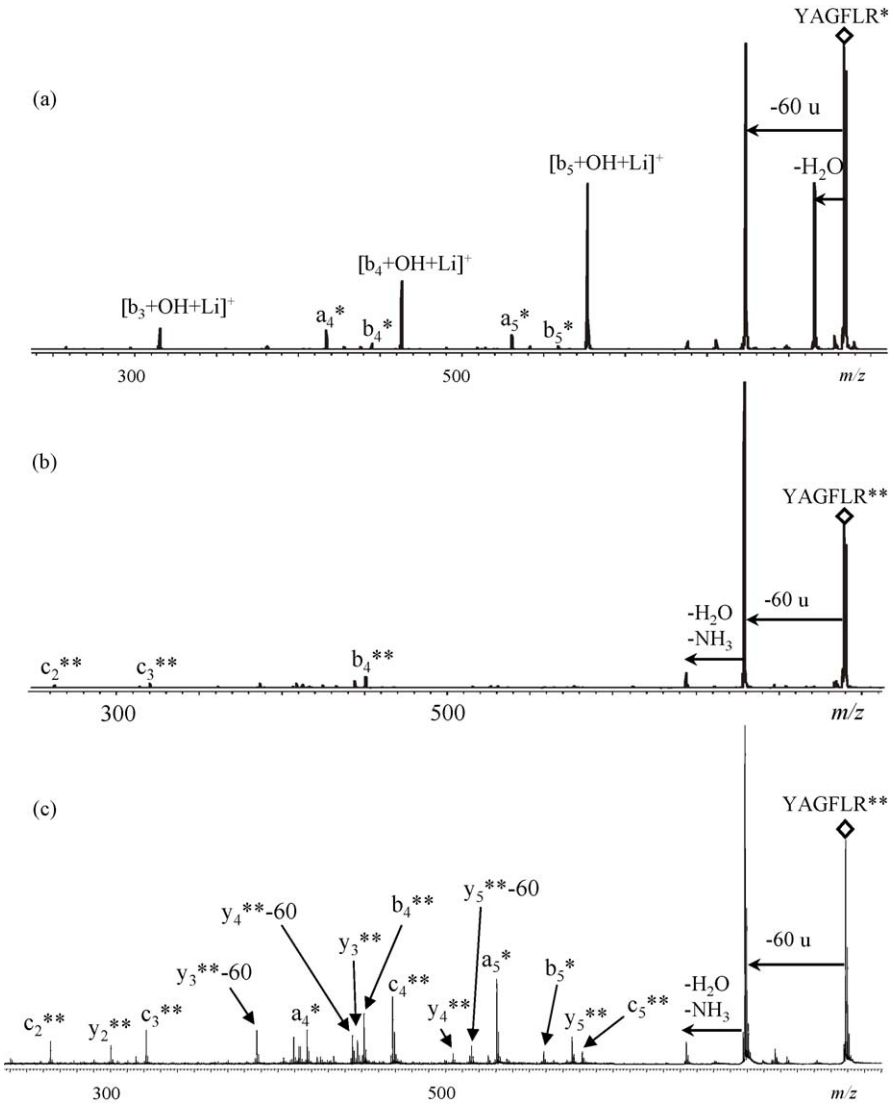

Fig. 8. CAD mass spectra of (a) $[YAGFLR + Li]^+$ (m/z 732) and (b and c) $[YAGFLR - H + 2Li]^+$ (m/z 738), acquired using (a and b) ESI-QIT and (c) MALDI-Q/ToF mass spectrometry. In part (c), the relative abundances of the peaks below m/z 600 have been magnified 4 times; this spectrum also shows a y_1^{**} ion (∼50% of y_2^{**}).

collisionally activated [53]; although many other fragments are formed, most of them have very low relative abundances and are difficult to interpret [53]. The loss of 60 u remains as the dominant decomposition pathway for the monolithiated forms of such peptides [54]; this is attested by the CAD spectrum of YAGFLR* in Fig. 8(a). The second most abundant fragment from the latter precursor ion is $[b_{n-1} + OH + Li]^+$, i.e., the fragment type usually dominating CAD spectra of lithiated peptides [24,32,42]. Monolithiated YAGFLR coproduces a few more members of the $[b_n + OH + Li]^+$ series, as well as select a_n^*/b_n^* ions, based on which partial sequence analysis is possible.

The dominant fragmentation pathway of singly charged dilithiated YAGFLR still involves the loss of 60 u, both under ESI-QIT and MALDI-Q/ToF tandem mass spectrometry conditions, cf. Fig. 8(b and c). More fragments and a better signal/noise ratio are obtained by CAD using the MALDI-Q/ToF than the ESI-QIT combination. In addition to the higher internal energies available by the former method (vide supra), the greater transmission efficiency of a ToF- versus a QIT-based mass analyzer also contributes to the larger number of detectable fragments in the Q/ToF vis à vis QIT tandem mass spectra. MALDI-Q/ToF CAD of $YAGFLR^{**}$ generates complete y_n^{**} and c_n^{**} series, which together with the select $y_n^{**}-60$ (characteristic of a C-terminal arginine residue [54]) and a_n^* ions observed, cf. (Fig. 8(c), provide sufficient information to deduce the peptide sequence.

It should be mentioned at this point that MALDI-ToF instrumentation is widely utilized for “peptide mapping” of tryptic digests, which are composed of peptides with C-terminal Arg or Lys residues. MALDI generally leads to singly charged ions. Very often, singly protonated peptides with Lys or Arg at their C-termini do not produce the sequence ions necessary for unequivocal sequence analysis. Dilithiation, coupled with MS/MS of the in situ generated Pep^{**} derivatives, can provide the desired information, as indicated by the data presented in Figs. 5(b) and 8 (b and c).

4. Conclusions

A wide range of singly charged dilithiated peptides has been studied by tandem mass spectrometry methods on both ESI-QIT and MALDI-Q/ToF instruments. In this type of peptide derivatives, a proton in the peptide is replaced by a lithium cation (usually at the most acidic site); the other lithium cation provides the charge and probably becomes mobile upon excitation, attaching at various locations of the peptide backbone, where it can induce fragmentation to produce sequence ions.

Theoretical calculations on the dipeptide complex $[FG - H + 2Li]^+$ found several different low-energy isomers for dilithiated FG. From the five structures calculated, the lithiated Li-carboxylate structures **1** and **2** are the most stable ones and very close in energy (**1**, 0 kJ/mol; **2**, +3 kJ/mol). The structures next lowest in energy are the lithiated Li-amide structures **3** (+33 kJ/mol) and **4** (+36 kJ/mol). The highest energy is found for the protonated Li-carboxylate and Li-amide structure **5** (+41 kJ/mol). Since the energy differences are not significantly large, all of these structures can be sampled during CAD.

Detailed examination of the MS/MS fragmentations of dilithiated peptides showed that such precursor ions can be very useful in the elucidation of peptide sequences. The study of a series of tripeptides further indicated that fragmentation at the C-terminal side of glycine residues does not take place efficiently and may be completely absent. CAD of the singly charged dilithiated peptides leads to almost complete structurally diagnostic y_n^{**}, c_n^{**} and a_n^{*} ion series.

The dissociations of $[Pep - H + 2Li]^+$ are consistent with the presence of salt bridges with both carboxylate and deprotonated amide structures in the fragmenting ion population, as predicted by theory (vide supra). These structures are found to promote sequence-specific decompositions as well as the elimination of radicals to form dilithiated peptide α-backbone radicals. As a whole, the (in situ) derivatized singly charged dilithiated peptides appear to be a promising alternative to protonated peptides in sequence analyses. Pep^{**} precursor ions would be most effective in sequence determinations of peptides whose protonated ions do not render sequence informative tandem mass spectra.

Acknowledgements

Generous financial support from the National Science Foundation (CHE-0111128) and the Ohio Board of Regents is gratefully acknowledged.

References

[1] K. Biemann, Methods Enzymol. 193 (1990) 455.
[2] M. Kinter, N.E. Sherman, Protein Sequencing and Identification Using Tandem Mass Spectrometry, Wiley-Interscience, New York, 2000.
[3] G. Siuzdak, The Expanding Role of Mass Spectrometry in Biotechnology, MCC Press, San Diego, 2003.
[4] W.J. Henzel, T.M. Billeci, J.T. Stults, S.C. Wong, C. Grimley, C. Watanabe, Proc. Natl. Acad. Sci. U.S.A. 90 (1993) 5011.
[5] A. Shevchenko, M. Wilm, O. Vorm, M. Mann, Anal. Chem. 68 (1996) 850.
[6] M. Barber, R.S. Bordoli, R.D. Sedgwick, A.N. Tyler, Nature 293 (1981) 270.
[7] Yoshida, K. Tanaka, Y. Ido, S. Akita, Y. Yoshida, Shitsuryo Bunseki 36 (1988) 59.
[8] M. Karas, F. Hillenkamp, Anal. Chem. 60 (1988) 2299.
[9] J.B. Fenn, M. Mann, C.K. Meng, S.F. Wong, Science 246 (1989) 64.
[10] P. Wang, M.M. Kish, C. Wesdemiotis, in: R.M. Caprioli, M.L. Gross (Eds.), The Encyclopedia of Mass Spectrometry, vol. 2: Biological Applications (Part A: Peptides and Proteins), Elsevier, 2004, p. 139.
[11] B. Paizs, S. Suhai, Mass Spectrom. Rev. 24 (2005) 508.
[12] A.R. Dongré, J.L. Jones, Á. Somogyi, V.H. Wysocki, J. Am. Chem. Soc. 118 (1996) 8365.
[13] M.J. Polce, D. Ren, C. Wesdemiotis, J. Mass Spectrom. 35 (2000) 1391.
[14] V.H. Wysocki, G. Tsaprailis, L.L. Smith, L.A. Breci, J. Mass Spectrom. 35 (2000) 1399.
[15] P. Roepstorff, J. Fohlman, Biomed. Mass Spectrom. 11 (1984) 601.
[16] K. Biemann, Biomed. Environ. Mass Spectrom. 16 (1988) 99.
[17] B. Paizs, S. Suhai, Rapid Commun. Mass Spectrom. 16 (2002) 375.
[18] B. Paizs, S. Suhai, A.G. Harrison, J. Am. Soc. Mass Spectrom. 14 (2003) 1454.
[19] B. Paizs, S. Suhai, J. Am. Soc. Mass Spectrom. 15 (2004) 103.
[20] T. Yalcin, C. Khouw, I.G. Csizmadia, M.R. Peterson, A.G. Harrison, J. Am. Soc. Mass Spectrom. 6 (1995) 1165.
[21] T. Yalcin, I.G. Csizmadia, M.R. Peterson, A.G. Harrison, J. Am. Soc. Mass Spectrom. 7 (1996) 233.
[22] M.M. Cordero, J.J. Houser, C. Wesdemiotis, Anal. Chem. 65 (1993) 1594.
[23] S.-W. Lee, H.S. Kim, J.L. Beauchamp, J. Am. Chem. Soc. 120 (1998) 3188.
[24] M.M. Kish, C. Wesdemiotis, Int. J. Mass Spectrom. 227 (2003) 191.
[25] W. Yu, J.E. Vath, M.C. Huberty, S.A. Martin, Anal. Chem. 65 (1993) 3015.
[26] J. Qin, B.T. Chait, J. Am. Chem. Soc. 117 (1995) 5411.
[27] R.A. Jockusch, P.D. Schnier, W.D. Price, E.F. Strittmatter, P.A. Demirev, E.R. Williams, Anal. Chem. 69 (1997) 1119.
[28] G. Tsaprailis, Á. Somogyi, E.N. Nikolaev, V.H. Wysocki, Int. J. Mass Spectrom. 195/196 (2000) 467.
[29] D.H. Russell, E.S. McGlohon, L.M. Mallis, Anal. Chem. 60 (1988) 1818.
[30] G. Renner, G. Spiteller, Biomed. Environ. Mass Spectrom. 15 (1988) 75.
[31] X. Tang, W. Ens, K.G. Standing, J.B. Westmore, Anal. Chem. 60 (1988) 1791.
[32] R.P. Grese, R.L. Cerny, M.L. Gross, J. Am. Chem. Soc. 111 (1989) 2835.
[33] J.A. Leary, T.D. Williams, G. Bott, Rapid Commun. Mass Spectrom. 3 (1989) 192.
[34] J.A. Leary, Z. Zhou, S.A. Ogden, T.D. Williams, J. Am. Soc. Mass Spectrom. 1 (1990) 473.
[35] R.P. Grese, M.L. Gross, J. Am. Chem. Soc. 112 (1990) 5098.
[36] L.M. Teesch, J. Adams, J. Am. Chem. Soc. 113 (1991) 812.
[37] P. Hu, M.L. Gross, J. Am. Chem. Soc. 114 (1992) 9163.
[38] J.A. Loo, P. Hu, R.D. Smith, J. Am. Soc. Mass Spectrom. 5 (1994) 959.
[39] J. Wang, R. Guevremont, K.W.M. Siu, Eur. Mass Spectrom. 1 (1995) 171.
[40] T. Lin, G.L. Glish, Anal. Chem. 70 (1998) 5162.
[41] B.A. Cerda, L. Cornett, C. Wesdemiotis, Int. J. Mass Spectrom. 193 (1999) 205.
[42] J.M. Barr, M.J. Van Stipdonk, Rapid Commun. Mass Spectrom. 16 (2002) 566.
[43] W.Y. Feng, S. Gronert, K.A. Fletcher, À. Warres, C.B. Lebrilla, Int. J. Mass Spectrom. 222 (2003) 117.
[44] F. Pingitore, C. Wesdemiotis, Anal. Chem. 77 (2005) 1796.
[45] P. Wang, C. Wesdemiotis, Proceedings of the 53rd ASMS Conference on Mass Spectrometry, San Antonio, Texas, June 5–9, 2005.
[46] M.J. Frisch, Gaussian-98, Rev. A9, Gaussian Inc., Pittsburgh, 1995.
[47] R.C. Dunbar, J. Phys. Chem. A 104 (2000) 8067.

[48] M.M. Kish, G. Ohanessian, C. Wesdemiotis, Int. J. Mass Spectrom. 227 (2003) 509.
[49] P.J. Linstrom, W.G. Mallard (Eds.), NIST Chemistry WebBook, NIST Standard Reference Database Number 69, June 2005. National Institute of Standards and Technology, Gaithersburg MD, 20899 (http://webbook.nist.gov).
[50] M.B. Smith, J. March, Advanced Organic Chemistry: Reactions, Mechanisms, and Structures, Wiley, New York, 2001.
[51] Y. Huang, J.M. Triscari, G.C. Tseng, L. Pasa-Tolic, M.S. Lipton, R.D. Smith, V.H. Wysocki, Anal. Chem. 77 (2005) 5800.
[52] A. Reiter, L. Teesch, H. Zhao, J. Adams, Int. J. Mass Spec. Ion Processes 127 (1993) 12.
[53] M.J. Deery, S.G. Summerfield, A. Buzy, K.R. Jennings, J. Am. Soc. Mass Spectrom. 8 (1997) 253.
[54] X.J. Tang, P. Thibault, R.K. Boyd, Org. Mass Spectrom. 28 (1993) 1047.